

Experimental and Numerical Studies of Dielectric Properties of BaTiO₃-platinum Composites at Microwave Frequencies

Yasuo Kuga, Seung-Woo Lee

Department of Electrical Engineering
University of Washington, Box 352500
Seattle, WA 98195, USA

Minoru Taya

Department of Mechanical Engineering
University of Washington, Box 352600
Seattle, WA 98195, USA

Abdulkhikim Almajid

Mechanical Engineering Department
King Saud University, Saudi Arabia

Sangil Lee

Electronics Engineering Department
Mokpo National University, Chonnam, Korea

Jing-Feng Li

State Key Laboratory of New Ceramics and Fine Processing
Department of Materials Science and Engineering
Tsinghua University, Beijing, 100084 P. R. China

and Ryuzo Watanabe

Department of Materials Processing
Tohoku University, Sendai, Japan

ABSTRACT

The conductor loading method has been used for creating a lossy dielectric material with a desired loss tangent. This method may also be applicable for developing high dielectric constant materials. In this paper, we will present the experimental results of the dielectric properties of BaTiO₃ and BaTiO₃-platinum (BaTiO₃-Pt) composites. These composite materials were designed to increase the real part of the effective dielectric constant at high frequency. Three different platinum volume fractions were used, 3, 5 and 10%, to make BaTiO₃-Pt composites, in addition to a pure BaTiO₃ material. To characterize the BaTiO₃-Pt composites, microwave frequency measurements were conducted using the waveguide transmission technique. The experimental and numerical results verify that it is possible to increase the dielectric constant using the conductor loading method.

Index Terms — Microwave dielectric properties, conductor loading, barium tetratitanate.

1 INTRODUCTION

HIGH relative dielectric constant (ϵ_r) materials such as barium-tetratitanate ($\epsilon_r = 37$ at 6 GHz) are often used for wireless devices as a substrate of miniature-sized antennas and dielectric resonators [1]. The typical

antenna has a dimension such as patch length and line length of approximately $\lambda/2$ to $\lambda/4$ where λ is the effective wavelength due to the substrate material or structure. Because most wireless systems operate at a lower microwave region, one technique to reduce the physical dimension is to fabricate antennas on a high ϵ_r substrate or resonator. The typical high- ϵ_r substrate materials are titania ($\epsilon_r = 96$ at 6 GHz) based composites and ϵ_r ranges

from 30 to 100. These dielectric materials also have relatively low loss characteristics at microwave frequencies. Although some materials such as strontium titanate (SrTiO₃) have very high ϵ_r (2000 to 4500 within a limited temperature range), they have limited use as an antenna substrate due to the requirement of a precise temperature control.

It is known that when dielectric materials are loaded with conducting particles, both the real and imaginary parts of ϵ_r will increase as the fractional volume of inclusion increases [3, 4]. This technique has been used for designing lossy dielectric materials such as beryllia-silicon carbide (BeO-SiC) and AlN-SiC for microwave tube applications [2]. The undoped beryllia (BeO) has a dielectric constant close to 6.4 and small loss tangent at the GHz region. When BeO is doped with SiC, the resulting composite materials show much higher real and imaginary parts of ϵ_r . The BeO-SiC composite is designed to absorb electromagnetic waves, and one of the requirements is high loss tangent which can be controlled by the amount of SiC.

The conductor loading method may also be applicable for creating high- ϵ_r materials. However, the main problem is that when the low-loss host material is loaded with conducting particles, both real and imaginary parts of ϵ_r tend to increase. The rate of increase depends on the volume fraction, size and shape, and conductivity of inclusions. Extensive analytical and numerical studies on the dielectric properties of composite materials have been conducted in the past, but there is no accurate model to predict the complex dielectric constant [4-7]. Moreover, there is very little published experimental data to compare with calculations. In this paper, we will present the experimental results of the dielectric properties of conductor-loaded composite materials.

2 MATERIAL PROCESSING

As we stated previously, our objective is to create a material with a very high dielectric constant using the conductor loading technique. Because the expected increase is 10 to 100% depending on the amount of inclusion and the volume fraction of the conductor cannot be too high because it will introduce conductor loss, the host material must have a high dielectric constant with a low-loss tangent. Barium titanate oxide (BaTiO₃) which has an $\text{Re}(\epsilon_r)$ of 90-110 and loss tangent of 0.001 is a good candidate, and this was chosen as a host material [10]. The conductivity of the inclusion material must be sufficiently high to minimize the conductor loss at microwave frequencies. In addition, conducting particles must withstand the high-temperature and high-pressure processing. Although silver, gold and copper are excellent conductors, they don't meet the other requirements. We chose platinum as the inclusion material. The conductivity of platinum [$\sigma = 9.52 \times 10^6$ (S/m)] is less than that of gold [$\sigma = 4.098 \times 10^7$

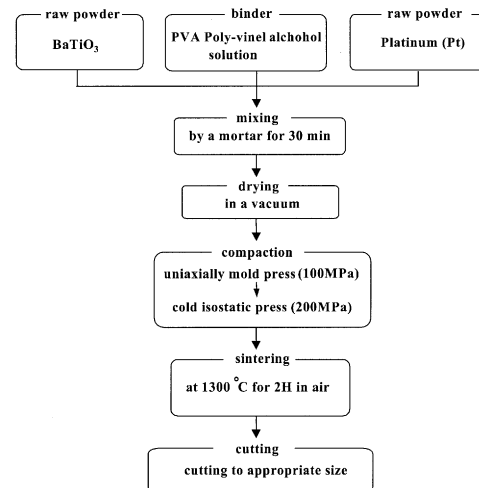


Figure 1. Flow chart of processing procedure.

(S/m)], but the material is suited for the high temperature processing.

Barium titanate oxide (BaTiO₃) ceramics and BaTiO₃ platinum (Pt) composites are fabricated by sintering powder compacts of BaTiO₃ and platinum. Predetermined amounts of BaTiO₃ powders were mixed with platinum powders in a mortar with a pestle. The fabrication procedures (flow chart) of the porous piezoelectric materials are shown in Figure 1. The starting material (BaTiO₃ powder, platinum, and PVA binder (poly-vinyl alcohol) are mixed by a mortar for 30 minutes. The mixture is then dried in a vacuum. Two stages of powder compaction are carried out, uniaxial pressing under 100 MPa to form the green samples and cold isostatic pressing under 200 MPa. The samples are then sintered at 1300° C for 2 h in air. The samples are then machined to the required dimensions for experimental investigation.

The sintered density of the composites is then determined. After sintering at 1300° C for 2 h, the powder compact is sintered to near full density. The BaTiO₃ platinum composites processed have 0, 3, 5, and 10 volume percent of platinum. The microstructures of the composites are observed using a scanning electron microscope (SEM) as shown in Figure 2. The white pores are the spaces that were occupied by the platinum particles. The size distribution of platinum particles is quite large as shown in Figure 2. Finally, the sample is cut into an X-band dimension and polished (Figure 3).

3 WAVEGUIDE DIELECTRIC CONSTANT MEASUREMENT TECHNIQUE

There are several different techniques to measure the dielectric constant of materials at microwave frequencies. If a sample can fit inside a waveguide or coaxial line, the most commonly used method is the Nicolson-Ross method

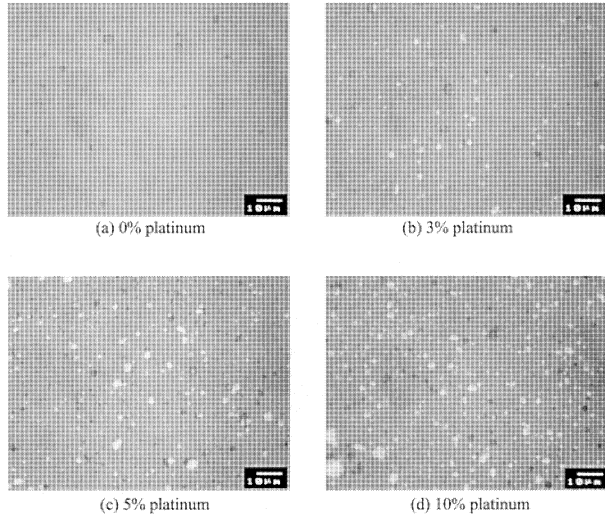


Figure 2. Micro-structural view of BaTiO₃ platinum composites.

and its variations which improves the stability for the sample length as it becomes close to $\lambda/2$ [8, 9]. Recently, we have developed a robust waveguide method to characterize lossy dielectric materials at X- (8.2–12.4 GHz) and S (2.6–3.9 GHz) bands [3]. The same setup and processing method will be used for this project.

The sample is placed inside the X-band waveguide, and the scattering parameters (S parameters) of the sample are obtained with the vector network analyzer (NWA) as shown in Fig. 3. This is the layered structure problem in which the material properties ϵ_r and μ_r are included in the characteristic impedance Z_s and propagation constant γ . S_{11} (reflection) and S_{21} (transmission) of the incident wave can be expressed with the following equations [1, 2].

$$\begin{aligned}\Gamma_1 &= \frac{Z_S - Z_0}{Z_S + Z_0} \\ \Gamma_2 &= \frac{Z_0 - Z_S}{Z_0 + Z_S} = -\Gamma_1 \\ \Gamma_3 &= \frac{Z_0 - Z_S}{Z_0 + Z_S} = \Gamma_2 = -\Gamma_1 \\ T_{21} &= 1 + \Gamma_1 \\ T_{12} &= 1 + \Gamma_2 = 1 - \Gamma_1\end{aligned}$$

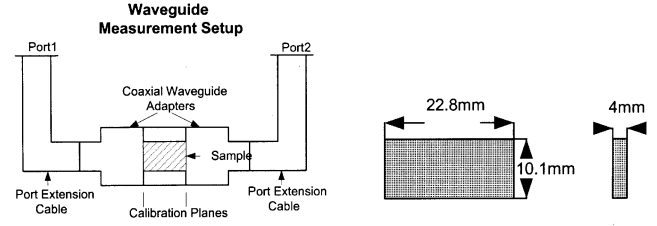
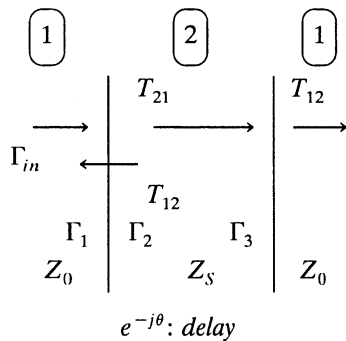


Figure 3. Left: Permittivity measurement setup with the waveguide sample holder; Right: Processed X-band waveguide sample size.

The total reflection S_{11} can be expressed as a summation of all reflections.

$$S_{11}(\omega) = \Gamma_1 + T_{12}T_{21}\Gamma_3 e^{-2j\theta} \sum_{n=0}^{\infty} \Gamma_2^n \Gamma_3^n e^{-2jn\theta} \quad (1)$$

Since $\sum_{n=0}^{\infty} x^n = \frac{1}{1-x}$ for $|x| < 1$, we get

$$S_{11}(\omega) = \Gamma_1 + \frac{T_{12}T_{21}\Gamma_3 e^{-2j\theta}}{1 - \Gamma_2\Gamma_3 e^{-2j\theta}} = \frac{\Gamma_1(1 - e^{-2j\theta})}{1 - \Gamma_1^2 e^{-2j\theta}} \quad (2)$$

Similarly, we can find S_{21} as

$$S_{21}(\omega) = T_{21}T_{12}e^{-j\theta} \frac{1}{1 - \Gamma_3\Gamma_2 e^{-2j\theta}} = \frac{(1 - \Gamma_1^2)e^{-j\theta}}{1 - \Gamma_1^2 e^{-2j\theta}} \quad (3)$$

where the phase shift θ is given by $\theta = \gamma L$ and L is the sample thickness. The wave number in the direction of wave propagation, γ , is given by

$$\gamma = \sqrt{\frac{\omega^2 \mu_r \epsilon_r}{c_0^2} - \left(\frac{2\pi}{\lambda_c}\right)^2} \quad (4)$$

where c_0 is a speed of light and λ_c is the cutoff wavelength of X band waveguide ($\lambda_c = 4.573$ cm).

The material properties μ_r and ϵ_r are included in the reflection coefficient Γ_j and γ in equations (2) and (3). In principle, both μ_r and ϵ_r can be obtained from S_{11} and S_{21} . If the sample material is non-magnetic ($\mu = \mu_0$), the permittivity ϵ_r has two unknowns, a real and an imaginary part, so that two equations are generally needed to solve the problem. Either S_{11} or S_{21} (complex variables) can be used to calculate ϵ_r . However, most experimental data contain random and systematic errors, and we have found that the S_{11} method is susceptible to a small amount of error in experimental data. Because of this concern, the inversion based on S_{11} was not used. The most robust approach to estimate ϵ_r is to measure S_{21} of the same material with two different thicknesses. By combining two S_{21} measurements and solving for one ϵ_r , it is possible to decrease the measurement uncertainty and increase the accuracy. Unfortunately, we have only one sample thickness in this project and the data inversion was conducted with one S_{21} data.

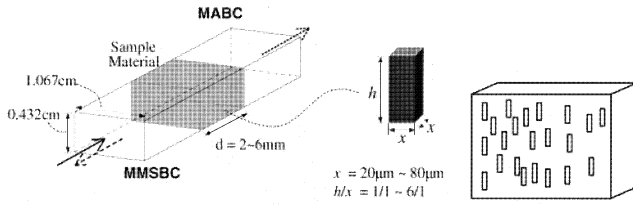


Figure 4. Configuration used for the FDTD simulations. The dimension of conducting particles and distributions in a sample (random case) are also shown.

4 FDTD SIMULATIONS OF BaTiO₃ COMPOSITE AND INVERSION

The objectives of the numerical simulations are (1) to test whether the data inversion method works for BaTiO₃ composite and (2) to test the effects of the shapes and orientations of inclusions. Most of our previous experiences with dielectric constant measurement were either lossy (loss tangent = 0.3 to 0.5) or low-loss dielectric materials such as a Teflon composite. To test whether the X-band waveguide method is suited for BaTiO₃ composites, we conducted finite difference time domain (FDTD) simulations using homogeneous materials. The FDTD method has been widely used for high frequency applications and details can be found in many references [11]. The simulation structure is shown in Figure 4. A sample material is assumed to have the dielectric constant $\epsilon_r = 110-j1$ and thickness = 4 mm. Figure 5 shows both S_{11} and S_{21} responses in time-domain. Unlike lossy materials or low-loss materials, the time-domain responses of a BaTiO₃ sample contain long tails. In most microwave frequency systems, small reflections from connectors and adapters are unavoidable. One of the nice features of modern NWA is a time-domain display which can be obtained from the original frequency-domain measurement. The location of large reflections can easily be identified in time-domain, and the time-domain gating function is usually employed to eliminate unwanted reflections. However, if a S_{21} time

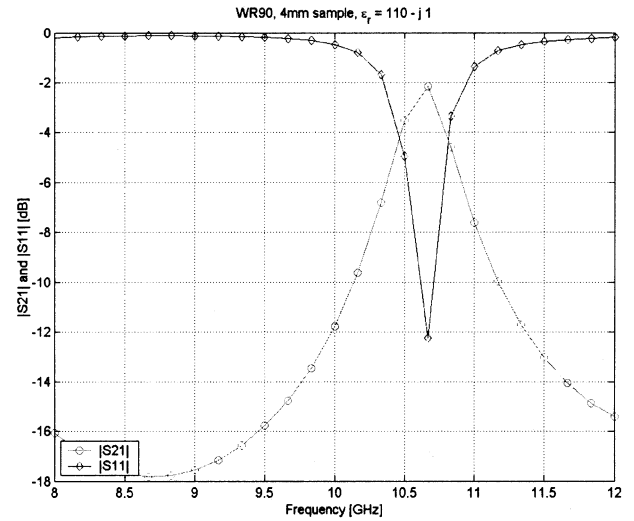


Figure 6. Frequency-domain responses of BaTiO₃ sample inside the X-band waveguide. Upper line S_{11} and lower line S_{21} . FDTD simulation. $\epsilon_r = 110-j1$ is used.

response has a long tail, it may be difficult to separate unwanted reflection from a desired response. The FDTD simulation provides the time-domain responses. To estimate the material properties, the time-domain response must be converted into the frequency-domain response and the inversion method such as genetic algorithm (GA) must be applied. Figure 6 shows the frequency-domain response of the same FDTD simulations. The correct value of ϵ_r was estimated from data shown in Figure 6 with equations (2) and (3). FDTD is a flexible method and, in principle, the different sizes and shapes of conducting particles can be included in a host BaTiO₃ in order to study their effects. In practice, however, the size of platinum particles cannot be too small due to the memory and CPU time requirements. Nevertheless, the FDTD simulations were conducted with two different particle shapes and the results will be discussed later.

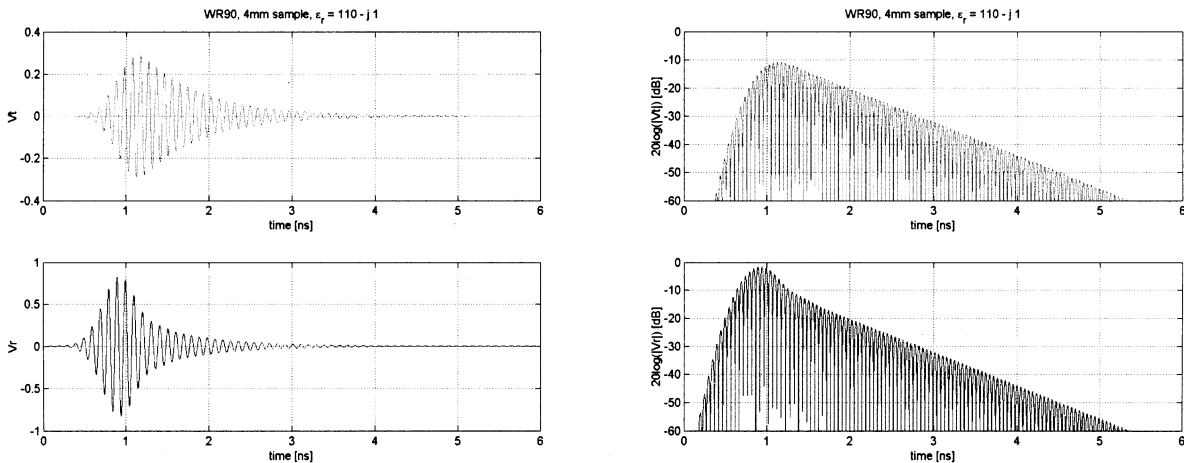


Figure 5. Time-domain responses of BaTiO₃ sample inside the X-band waveguide. Top S_{21} and bottom S_{11} . FDTD simulation. $\epsilon_r = 110-j1$ is used.

5 EXPERIMENTAL RESULTS

Figure 7 shows the S_{21} responses of the BaTiO₃ sample without platinum particles in both time- and frequency-domains. NWA is properly calibrated to obtain S_{21} data shown in Figure 7. The general trend is very similar to that of the FDTD simulation shown in Figures 5 and 6. As expected the time-domain response shows a long tail, and it is difficult to determine the optimum gate position. To isolate a desired response from the reflection caused by the waveguide-to-coaxial adapter, we also conducted the measurement with a long X-band waveguide, but there was no significant difference.

Figure 8 shows the time-domain responses of the BaTiO₃ composite with Pt = 3% and Pt = 10%, respectively. The inclusion of platinum does not change the shape significantly indicating that the loss part is still small in these samples. The gate position was chosen to select a desired response only. For example, the second large peak shown in the Pt = 0 and 3% cases (left figure in Figures 7

and 8) is a spurious reflection, and it must be eliminated before processing data. It appears that the Pt = 10% case (Figure 8, right) shows a longer tail compared to the Pt = 0% case. This can be explained in that the Pt = 10% case has a higher dielectric constant than that of Pt = 0%. Therefore, the energy will be trapped within the material longer than that of the Pt = 0% case.

The complex dielectric constants are estimated from the measured frequency domain S_{21} data shown in Figure 9 for four different platinum concentrations. The accuracy of the estimation depends on the random and systematic noises in the original S_{21} data. Based on previous experience, we have found that if the magnitude of S_{21} is greater than 0.2, the error in estimation is small. Figure 10 shows the estimated ϵ_r of four Pt concentrations. If we estimate ϵ_r with more controlled data of $|S_{21}| > 0.4$, the average value of effective dielectric constants are $\epsilon_r = 112$ for Pt = 0%; $\epsilon_r = 121$ for Pt = 3%; $\epsilon_r = 129$ for Pt = 5%; and $\epsilon_r = 146$ for Pt = 10%. The effective dielectric constant is

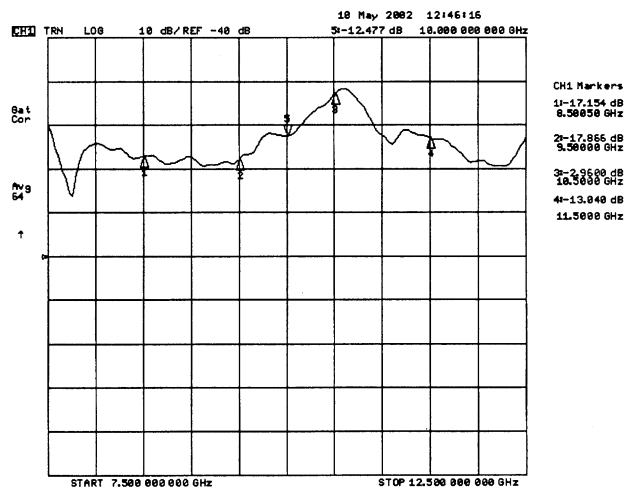
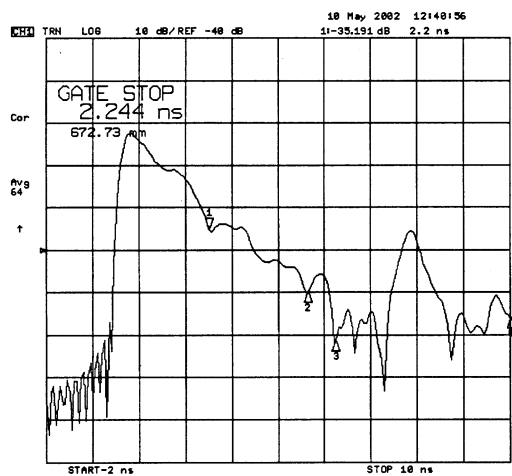


Figure 7. Time- and frequency-domain responses of BaTiO₃ sample (Pt = 0%). In frequency-domain, the gate width is set to -0.5 ns to 5.5 ns.

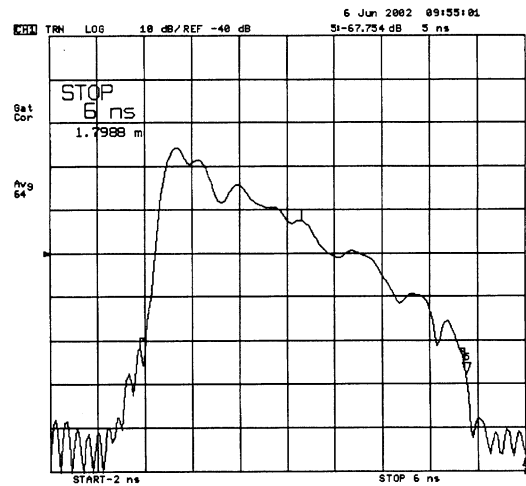
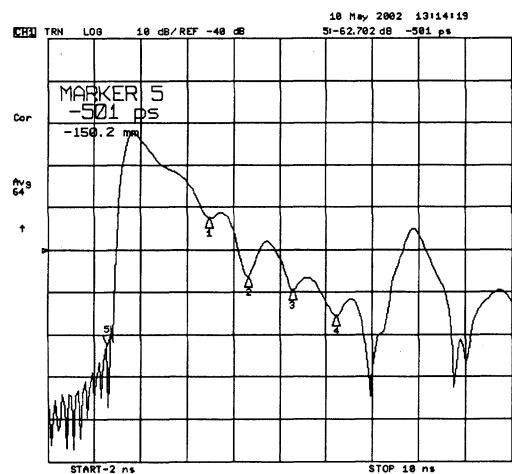


Figure 8. Time-domain responses of BaTiO₃ samples. Left, Pt = 3%; Right, Pt = 10%.

increased by 30% over this range. The waveguide transmission technique is not suited for measuring a small imaginary part accurately, and results of the imaginary part may contain significant error. However, the imaginary part does not increase much up to the platinum concentration of 10%. A better method to estimate the imaginary part is the cavity-based techniques.

In this experiment, we did not control the sizes and shapes of platinum particles, and most particles are found to be much smaller than 10 μm. To study the effects of particle sizes and shapes on the effective dielectric constant, we have conducted the FDTD simulations [12]. Figure 11 shows both real and imaginary parts of ε_r for four different aspect ratios. The size of base area (x by x) is fixed at 40 μm x 40 μm and the height (h) is changed from 40 to 240 μm. It is clear that by controlling the aspect ratio and orientation of particles, we may be able to increase the real part of the effective dielectric constant significantly. This has to be tested experimentally.

6 CONCLUSIONS

Although our results are still preliminary, we have shown that a higher dielectric constant can be achieved

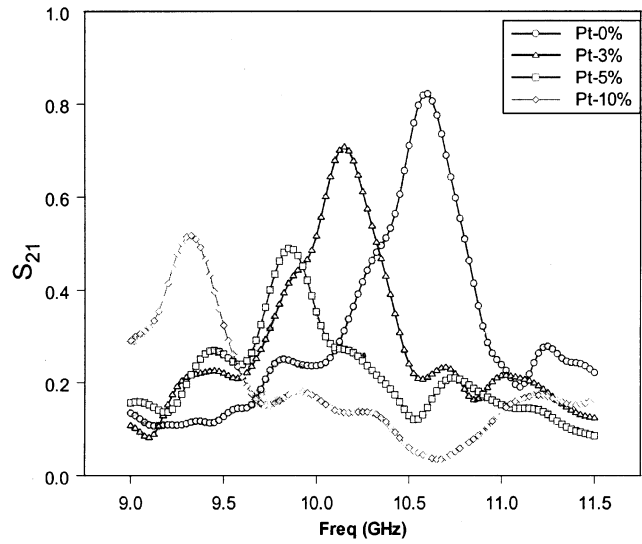


Figure 9. Magnitude of S₂₁ for four different Pt concentrations. Pt = 0%, Pt = 3%, Pt = 5%, Pt = 10%.

with the conductor loading technique. The increase is approximately 30-35% for the Pt = 10% case. Unlike lossy dielectric materials such as BeO-SiC, we have found that

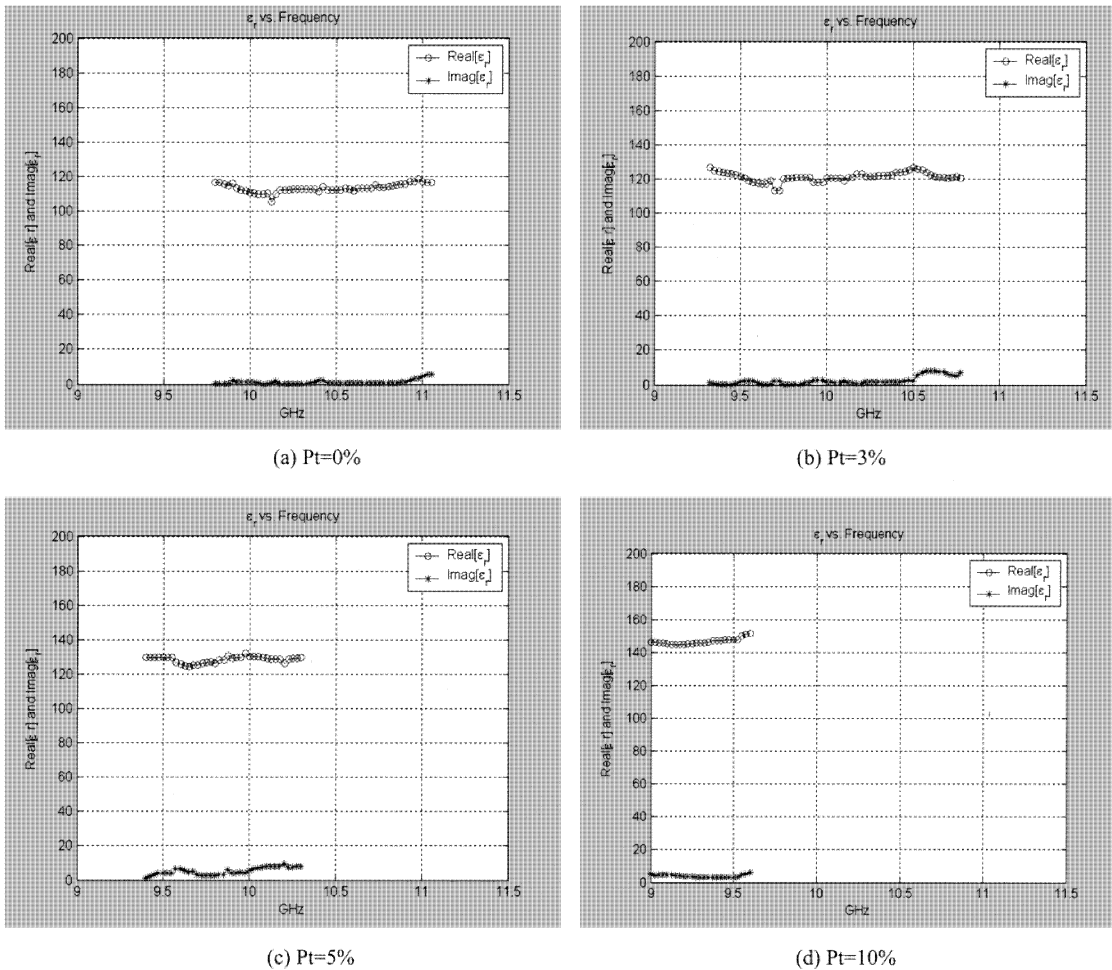


Figure 10. Estimated dielectric constant of BaTiO₃ composites for four different Pt concentrations.

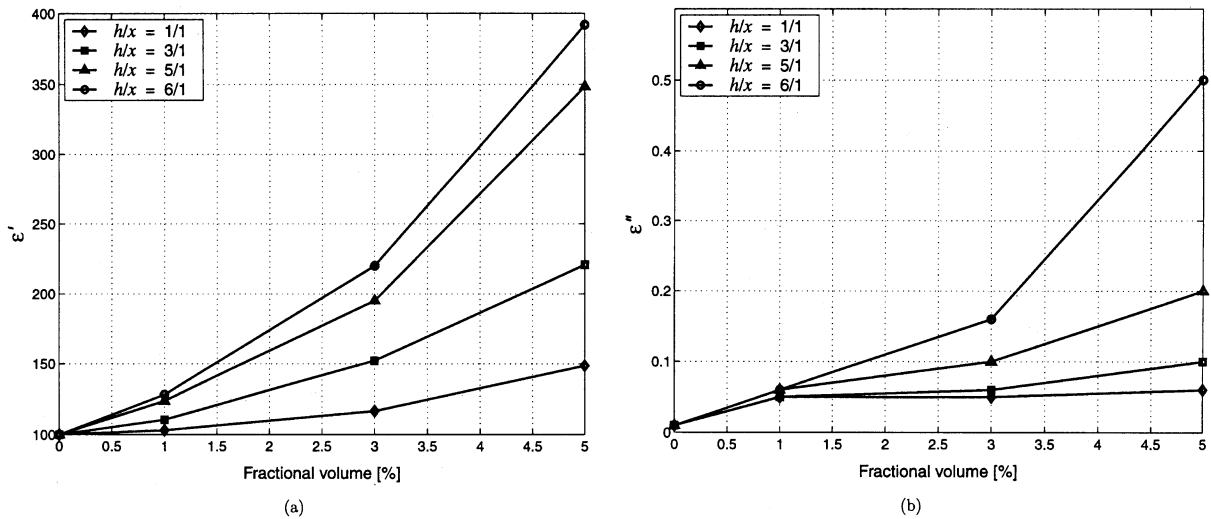


Figure 11. Real (left) and imaginary (right) part of ϵ_r versus fractional volume of conducting particles. Particles are perfect conductor with the base size of $x = 40 \mu\text{m}$. The host = $\epsilon_r = 100 - j0.01$, frequency = 2.2 GHz. The particle height h is varied to show the effects of aspect ratio (see Figure 4).

the high ϵ_r and low loss materials pose problems in both measurements and data inversion process. The instability encountered in the inversion process may be due to the inaccurate data obtained from NWA. The gate position and width as well as the material placement are critical in this experiment. Although a silver paint was used for plugging small air gaps between the sample and waveguide, another source of error in measurements is these small air gaps. Finally, the FDTD numerical simulations show that a further enhancement of dielectric constant is feasible by controlling the particle aspect ratio and orientation.

ACKNOWLEDGMENTS

This work is supported by the National Science Foundation (ECS-9908849).

REFERENCES

- [1] S. J. Fiedziuszko, I. C. Hunter, T. Itoh, Y. Kobayashi, T. Nishikawa, S. N. Stitzer, and K. Wakino, "Dielectric Materials, Devices, and Circuits", IEEE Trans. Microwave Theory Tech., Vol. 50, pp. 706–720, 2002.
- [2] D. Abe, "IVEC Summary Session 3, Materials I", Third IEEE International Vacuum Electronics Conference (IVEC) Monterey, CA, 2002.
- [3] S. Lee, Y. Kuga, and E. Savrun, IEEE AP-S/URSI Symposium, Salt Lake City, Utah, p. 63, 2000.
- [4] W. T. Doyle, "Particle Clustering and Dielectric Enhancement in Percolating Metal-insulator Composites", J. Appl. Phys., Vol. 78, pp. 6165–6169, 1995.
- [5] P. S. Neelakanta, "Microwave Absorption by Conductor-loaded Dielectrics", IEEE Trans. Microwave Theory Tech., Vol. 43, pp. 1381–1383, 1995.
- [6] M. Taya, *Electronic Composites*, Cambridge University Press, 2005, in press.
- [7] D. S. McLachlan, A. Priou, I. Chenerie, E. Issac, and F. Henry, "Modeling the Permittivity of Composite Materials with a General Effective Medium Equation", J. of Electromagnetic Waves and Applications, Vol. 6, pp. 1099–1131, 1992.

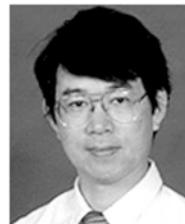
[8] Agilent (HP) product note 8510-3.

[9] J. Baker-Jarvis and E. J. Vanzura, "Improved Technique for Determining Complex Permittivity with the Transmission/Reflection Method," IEEE Trans. MTT, Vol. 38, pp. 1096–1101, 1990.

[10] D. M. Pozar, *Microwave Engineering*, Wiley, 2003.

[11] A. Taflov, *Advances in Computational Electrodynamics: The Finite-Difference Time-Domain Method*, Artech House, MA, 1998.

[12] S.-W. Lee, *Computational Electromagnetic Applications for the Analysis of Rough Surface Scattering and Artificial Composite Materials*, Ph.D. Thesis, University of Washington, Seattle, WA 2002.



Yasuo Kuga (F'04) is a Professor of Electrical Engineering at the University of Washington. He received the B.S., M.S., and Ph.D. degrees from the University of Washington, Seattle in 1977, 1979, and 1983, respectively. From 1983 to 1988, he was a Research Assistant Professor of Electrical Engineering at the University of Washington. From 1988 to 1991, he was an Assistant Professor of Electrical Engineering and Computer Science at The University of Michigan. Since 1991, he has been with the University of Washington. He was an Associate Editor of Radio Science (1993-1996) and IEEE Trans. Geoscience and Remote Sensing (1996-2000). His research interests are in the areas of microwave and millimeter-wave remote sensing, high frequency devices and materials, and optics.



Sang-il Lee received the B.E. and M.E. degrees in electronics engineering from Korea University, Seoul, Korea, and the Ph.D. degree in electrical engineering from the University of Washington, Seattle, WA in 1991, 1994, and 2002, respectively. He joined Samsung Electronics in 2002, where he worked on fiber-based wireless indoor networks. In 2003, He joined the faculty of the department of Electronics Engineering, Mokpo National University, Korea. His main research interests are in the fields of microwave techniques and broad-band communications.

Ryuzo Watanabe is at Tohoku University, Sendai, Japan.



Seung-Woo Lee is a Senior Engineer at Mobile Communication Division of Samsung Electronics. Co. Ltd., Suwon, Korea. He received the B.S. and M.S. degrees in electrical engineering from Seoul National University, Korea, in 1994 and 1996, respectively and the Ph.D. degree in electrical engineering from the University of Washington, Seattle in 2002. In 2003, he was a Research Associate of the Department of Electrical

Engineering at the University of Washington. His research interests include computational electromagnetics, rough surface and random media scattering, and RF circuit design and compact antennas for wireless communication.



Minoru Taya obtained the B.S. degree in engineering in 1968 from the University of Tokyo, and the M.S. and Ph.D. degrees in 1973 and 1977, respectively in theoretical applied mechanics from Northwestern University. Dr. Taya is currently Professor of Mechanical Engineering, and adjunct professor of Materials Science and Engineering and Electrical Engineering, at University of Washington. During 1989-1991, he served as

Professor of Materials Systems, Tohoku University, Department of Materials Processing. Since then, Dr. Taya has been working on smart materials and electronic composites as his main thrust research area. Dr. Taya is Fellow of ASME (1994) and American Academy of Mechanics (2000). Dr. Taya is currently running a Center for Intelligent Materials and Systems (CIMS; <http://depts.washington.edu/cims>) as Director. Dr. Taya has published over 250 papers including two books; M. Taya and R. J. Arsenault, *Metal Matrix Composites*, 1989, Pergamon Press, and M. Taya, *Electronic Composites*, Cambridge University Press, 2005 in press.



Abdulhakim Almajid was born in Riyadh, Saudi Arabia on 13 September 1969. He received the B.S. degree in mechanical engineering from King Saud University in 1991, and the M.S. degree in mechanical engineering from Washington University in St. Louis in 1995, and the Ph.D. degree in mechanical engineering from University of Washington in Seattle in 2002. Currently, he is an Assistant Professor at the Mechanical Engineering Department at King Saud University, Saudi Arabia. His research lies in smart materials and MEMS technologies, design and processing of piezoelectric devices. His research applications include microelectronics, transducers.



Jing-Feng Li received the B.S. degree in materials science and engineering from Huazhong University of Science and Technology, Wuhan, China, in 1984, and the M.S. and Ph.D. degrees in materials science and engineering from Tohoku University, Sendai, Japan in 1988 and 1991, respectively. He was Assistant Professor from 1992 to 1997 and Associate Professor from 1997 to 2002 in the Department of Materials Processing, Tohoku University. He is currently a Professor in the Department of Materials Science and Engineering, Tsinghua University, Beijing, China. His research interests include MEMS materials and micro-fabrication technology, piezoelectric ceramics, thermoelectric materials, functionally graded materials, advanced ceramics and ceramic composites.